Density-functional theory of the kinetics of crystallization of hard-sphere suspensions: Single conserved order parameter

Robert Wild and Peter Harrowell
School of Chemistry, University of Sydney, Sydney, New South Wales 2006, Australia
(Received 23 April 1997)

A theoretical study is presented of the kinetics of crystallization of a hard-sphere-like colloidal suspension in a fixed volume based upon the use of time-dependent density-functional theory incorporating conserved particle dynamics. Distinguishing crystalline order by the particle density alone, we demonstrate that the constraints of fixed number and volume lead naturally to the appearance of a new nonuniform minimum in the free energy corresponding the equilibrium coexistence between crystalline order and disordered suspension. Using numerical integration, we follow the time dependence of a range of initial spherical crystallites. The normal and tangential osmotic pressure fields about these growing crystallites are presented and the growing crystallite is shown to be isolated from the higher pressure of the surrounding disordered suspension by the nonequilibrium depletion zone which surrounds it. These results are compared with recent light-scattering studies. [S1063-651X(97)06409-X]

PACS number(s): 64.70.Dv, 81.10.Fq, 82.70.Dd

I. INTRODUCTION

In this paper we present a theoretical study of the kinetics of crystallization of a hard-sphere-like colloidal suspension in a fixed volume based upon the use of time-dependent density-functional theory, and incorporating conserved particle dynamics. The use of a microscopic statistical theory allows us to describe the time-dependent cluster structure and local pressures, transient depletion zones, and stationary states all within a single consistent theoretical framework.

Crystallization in a fixed volume introduces a complication into the standard picture of crystal growth. Due to the density difference between crystal and liquid, crystal growth is accompanied by an inevitable change in the thermodynamic states of both phases. In the case of sterically stabilized colloidal suspension, the crystal has a higher density than the disordered suspension and, consequently, crystal growth is accompanied by a general decrease in the osmotic pressure of the two-phase system. One of the central theoretical concerns of this paper is the consistent treatment of crystal growth in the presence of a time-varying thermodynamic state.

In considering the nature of the inhomogeneities in the crystallizing suspension, we must also take into account the diffusive character of colloidal particle motion. In the case of pure atomic or molecular liquids, a transient local-density depletion can be rapidly relaxed by longitudinal modes, a process typically much faster than crystal growth itself. In the case of colloidal suspensions, relaxation of such a local-density depletion, along with gradients in the osmotic pressure, are relaxed via diffusive motion of particles. As this relaxation typically takes place on time scales similar to that of crystallization, any theoretical description of crystal growth in colloids must take into account the possibility of nonequilibrium density and osmotic pressure gradients. This feature will be treated in detail in the analysis presented below.

A number of light-scattering studies[1–5] have been carried out on suspensions of silica or polystyrene particles stabilized by polymers bound to the surface. (In the case of ref. [1], the particles also carried a slight charge.) The equilibrium structure factor and freezing transition are found to be in reasonable quantitative agreement with those of the hard-sphere liquid (with the use of an effective hard-sphere diameter), and we shall make extensive use of the analogy with hard sphere liquids in the course of this paper. Low-angle light scattering [2,3] has been used to measure the size of growing crystal clusters, making use of the concentration difference between crystal and liquid. Scattering from sets of crystal planes (high angle or Bragg scattering) have also been measured [1,4,5]. The intensity of the scattering provides a measure of the amount of crystalline material in the scattering volume, and the width of the scattering peak can be related to an average cluster size, while the magnitude of the wave vector of the peak is proportional to the inverse of the lattice spacing in the growing crystallites.

The variation of this last quantity during the course of crystallization, measured by Harland and van Megen (HvM) [5], provides us with an explicit characterization of the time-dependent state of the crystal, as opposed to simply the time dependence of the cluster size. As this novel feature is particular to crystallization under the constraint of fixed N and V we shall consider these results [5] in some detail. HvM observed the magnitude of the wave vector at the scattering peak decreasing monotonically in time for all volume fractions studied. The duration of this decrease is essentially equal to the time interval over which the total amount of crystal increases, consistent with the idea that the expansion of the crystal lattice is a direct reflection of the drop in the osmotic pressure of the disordered suspension due to crystallization. (Note that the crystalline peak is indistinguishable from the broad liquid scattering peak for very small crystallites. This limitation leaves a veil over the early history of the clusters.) Equating the decrease of the wave vector with a uniform increase in the dimension of the unit cell, HvM converted their peak shifts into monotonic decreases in the crystal volume fraction as crystallization proceeds. The initial

crystal volume fractions are significantly higher than the final value, indicating that the small clusters are under compression. For suspensions with a total concentration below the melting volume fraction, the final value of the crystal concentration is found to be equal to the melting volume fraction. In the case of samples at higher concentrations, the final crystal concentration does not quite fall to the expected final crystal volume fraction, i.e., that of the suspension itself. HvM attribute this to the slowness of the coarsening process.

The analysis can be extended by feeding this crystal volume fraction into an equation of state of the hard-sphere crystal to obtain a corresponding pressure, effectively using the crystal-lattice spacing as an *in situ* osmotic pressure gauge [5,6]. This approach neglects the complexity of defining pressure in the nonuniform suspension (see Sec. III below) but would be expected to provide sensible estimates in cases where the crystallite radius considerably exceeds the interfacial width. The osmotic pressure so obtained also exhibits a monotonic decrease in time. The initial crystal pressure is typically found to be less than that predicted for the disordered suspension (using an analogous liquid equation of state for hard spheres), which led HvM to suggest that the growing cluster is mechanically isolated, to some degree, from the bulk disordered suspension by a depletion zone.

Ackerson and Schätzel (AS) [3] recently examined a theoretical model of the crystallization process which addressed a number of these features of constrained crystallization. They considered the problem of a spherical crystal growing in a spherical volume of suspension, the latter surrounded by a no-flux boundary. The model consists of a crystal-liquid interface of zero width coupled to the concentration fields of the crystal and the disordered suspension. The interface is driven by the chemical potential difference between the ordered and disordered phases via the Wilson-Frenkel [7] growth law, modified to include a surface curvature contribution to the chemical potential difference. Number conservation is imposed, so that the density change on crystallization couples the motion of the interface to the transport of material in the adjacent phases. Particle transport in the crystal and disordered suspensions is described with simple Fick's law diffusion. The model exhibits a crossover in growth laws with increasing supercooling. At small supercoolings the crystal radius increases linearly with time, changing over to diffusion-controlled $t^{1/2}$ dependence at higher supercoolings. (Note that ''supercooling'' is used here to mean ''chemical potential difference between the crystal and disordered phase,'' and does not refer to the use of temperature to adjust the relative stability of the two phases.) AS also found that the density of the crystal at the cluster center generally underwent an initial rapid increase as the small crystallite was compressed by the surrounding suspension. This was followed by a steady density decrease, mirroring the drop in the osmotic pressure of the disordered suspension due to crystallization. The field theory we present in this paper differs from this earlier work in that the entire suspension, crystal, interface, and disorder, is treated within a single consistent formalism. The interface is allowed to ''adjust''its width, surface curvature contributions appear naturally instead of being explicitly inserted, and particle transport is driven by gradients of the local chemical potential rather than concentration gradients. One of the goals of this paper is to see how the crystallization predicted by the density-functional theory differs from the classical results of Ref. [3].

The paper is arranged as follows. The equation of motion is described in Sec. II, along with the boundary conditions. The formalism required to calculate the normal and tangential components of the pressure is presented in Sec. III. In Sec. IV we present the stationary solutions to this equation, demonstrating the constraint of fixed volume naturally results in two nonuniform stationary density profiles. The time-dependent behavior of the growing clusters is described in Sec. V, followed by a brief discussion of the insights on crystal nucleation provided by this work in Sec. VI. The paper concludes with a discussion in Sec. VII.

II. THEORETICAL MODEL

We are interested in the description of crystallization under conditions in which volume and particle number are conserved, i.e., crystallization in the ''canonical ensemble.'' This constraint is imposed through a zero-particle flux boundary condition. The central consequence of this constraint and the inherent concentration difference between the solid and liquid phases is that, as crystallization proceeds, particle concentration in the disordered suspension is depleted. This in turn results in a continuously varying state of the suspension, characterized by a time-dependent osmotic pressure, until growth finally ceases at coexistence.

We have chosen to consider the simplest representation of the solid-liquid transition which retains the concentration difference in order to clarify a consistent treatment of conserved dynamics under the constant V,N constraints. In this treatment, order and disorder are distinguished solely on the basis of concentration. The simplicity of this description comes with a price, we can no longer distinguish a dense metastable disordered suspension from the crystal of the same concentration and are reduced to nominating a crossover concentration ρ_c above which the system is regarded as crystalline. This means that we are restricted to studying crystallization from suspensions of concentrations no greater than ρ_c, a value which we have taken to be midway between the freezing and melting values. A study of crystallization at higher concentrations will be presented in a later paper, which will consider a structural order parameter in addition to the concentration.

The dynamics of the scalar field $\rho(\mathbf{r},t)$ is assumed to be governed by the following equation of motion;

$$\frac{\partial\rho(\mathbf{r},t)}{\partial t}=D\nabla^2\frac{\delta F}{\partial\rho(\mathbf{r})}. \tag{1}$$

The Laplacian ensures particle conservation as the dynamics deterministically advances the system toward the stationary states characterized by a uniform chemical potential $\mu=\delta F/\delta\rho(\mathbf{r})$. The free-energy functional $F[\rho]$ is the Helmholtz free energy as dictated by the canonical constraints of fixed N, V, and T. This choice of free energy requires some discussion. The standard choice of free energy in a partial functional differential equation like Eq. (1) is the grand-canonical free energy [8]. In the canonical ensemble the

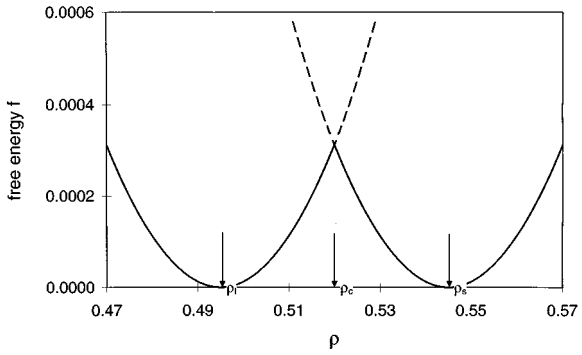

FIG. 1. The two-parabola approximation to the free energy $f(\rho)$ of a uniform system of particle density ρ. The solid, disordered, and crossover densities ρ_s, ρ_l, and ρ_c are indicated. Reduced units are defined in Sec. IV.

functional differentiation with respect to the density should include the density constraint, a difficulty avoided in the grand-canonical ensemble. In this treatment we have imposed the density constraint as a dynamical constraint through the boundary conditions (described below) and, hence, have neglected it in evaluating the functional derivatives.

The free energy functional is assumed to be of the square gradient form [9]

$$F=\int d\mathbf{r} f(\rho(\mathbf{r}))+\frac{\kappa}{2}(\nabla\rho(\mathbf{r}))^2. \tag{2}$$

The local free energy $f(\rho)$ is that of a uniform system characterized by the local concentration. Each uniform stable or metastable phase must appear as a minimum in this local free energy. We have chosen to represent $f(\rho)$ here by a double parabola (see Fig. 1),

$$f(\rho)=\min\left[\frac{\lambda_l}{2}(\rho-\rho_l)^2,\ \frac{\lambda_s}{2}(\rho-\rho_s)^2\right]. \tag{3}$$

For the uniform system we have the following expressions for the chemical potential μ and the osmotic pressure π:

$$\mu=\mu_0+\frac{df}{d\rho}, \tag{4}$$

$$\pi=\pi_0+\rho\frac{df}{d\rho}-f, \tag{5}$$

where μ_0 and π_0 are the chemical potential and osmotic pressure at crystal-disorder coexistence. Substituting the expression for the local free energy $f(\rho)$ into the expression for the osmotic pressure of the uniform system we find

$$\pi(\rho)=\pi_0+\frac{\lambda_\alpha}{2}(\rho^2-\rho_\alpha^2), \tag{6}$$

where the subscript $\alpha=l$ or s, depending on whether the concentration places us in the disordered or ordered phase. This approximate equation of state provides a reasonable fit to accurate empirical equations of state for the hard sphere liquid [10] and solid [11] over the limited concentration range accessible by the one order-parameter theory. Using reduced density units of $(3/4\pi)\sigma^{-3}$ (σ being the particle diameter) we have set $\rho_l=0.495$ and $\rho_s=0.545$. A satisfactory fit of the crystal and liquid pressure over the relevant density range was achieved with $\lambda_l=\lambda_S$.

The typical representation of supercooling in terms of the local free-energy function f is as the free-energy difference between the two local minima. So the metastability of the supercooled liquid, for example, is modeled by lowering the local minimum representing the solid by an amount which then becomes the control parameter in the model—the explicit measure of the free-energy difference between the two bulk phases. In the case of an athermal system like the hard-sphere liquid, however, the total density completely specifies the state—there is no additional independent intensive parameter such as temperature which can be used to adjust the relative free energies of the two phases. In light of this, the local free energy f used in this analysis is as pictured in Fig. 1 for all values of the total concentration. As we shall see, it is the constraint that the transition dynamics must conserve particle number which will render the bulk liquid minimum to be metastable for total concentrations greater than the freezing concentration ρ_l (or, to be exact, ρ_x as defined in Fig. 4).

The equation of motion is

$$\frac{\partial\rho}{\partial t}=D\nabla^2\left(\frac{df}{d\rho}-\kappa\nabla^2\rho\right). \tag{7}$$

We shall restrict our attention to the case of a spherical cluster confined within a volume of radius R. We assume that while flow of material within this spherical region is unconstrained, there is no flow of particles into or out of this region. The idea is to model (crudely) the effect of a growing cluster competing for material with similar clusters in neighboring regions. The neglect of transfer of particles from one cluster to another precludes us from investigating the slower process of coarsening in this work.

In spherical coordinates, the equation of motion is

$$\begin{aligned}\frac{\partial\rho(\mathbf{r},t)}{\partial t}&=D\frac{1}{r}\frac{\partial^2}{\partial r^2}\left(r\frac{\delta F}{\delta\rho(\mathbf{r},t)}\right)\\&=\frac{D}{r}\frac{\partial^2}{\partial r^2}\left(r\frac{df}{d\rho}-\kappa^2\frac{\partial^2\rho}{\partial r^2}\right).\end{aligned} \tag{8}$$

This equation of motion is first order in time and fourth order in the radius, and so requires one initial and four boundary conditions, respectively. We provide an initial profile $\rho_0(r)$ so that

$$\rho(r,0)=\rho_0(r). \tag{9}$$

The radial boundary conditions are as follows:

$$\left.\frac{\partial\rho(r,t)}{\partial r}\right|_{r=0}=0, \tag{10}$$

a result of the requirement that ρ be differentiable;

$$\left.\frac{\partial\rho(r,t)}{\partial r}\right|_{r=R}=0, \tag{11}$$

$$\left.\frac{\partial^3\rho(r,t)}{\partial r^3}\right|_{r=R}=0, \tag{12}$$

by virtue of the symmetry arising from the equivalence of neighboring volumes; and

$$\left.\frac{\partial^2\rho(r,t)}{\partial r^2}\right|_{r=R}=0, \tag{13}$$

the consequence of the previous conditions and the constraint of particle conservation.

III. CALCULATING THE NORMAL AND TANGENTIAL OSMOTIC PRESSURES OF THE GROWING CRYSTAL CLUSTER

The time dependence of the osmotic pressure during crystallization is the defining complication of crystallization in a fixed volume and, as demonstrated in Ref. [5], a valuable source of information in the analysis of the crystallization process. The deduction of the osmotic pressure from the observed lattice spacing of a growing crystallite, however, has its subtleties. Some of these have been indicated in the study by Ackerson and Schätzel [3]. In a finite spherical cluster the surface tension will provide a contribution to the pressure of the crystal. When a cluster radius is significantly larger than the interfacial width, the crystal pressure is well defined and, assuming mechanical equilibrium, we can write

$$\pi_{\text{solid}}=\frac{2\gamma}{R_c}+\pi_{\text{liquid}}, \tag{14}$$

where γ is the solid-liquid surface tension and R_c is the crystal radius. Mechanical equilibrium, however, is achieved in the colloidal suspension through the slow process of diffusion, and hence its establishment will be on the same time scale as the crystal growth itself. How valid then is the assumption of mechanical equilibrium? Furthermore, how should we relate crystal and liquid pressures for clusters of the same extent as the interfacial width? Can we define inhomogeneous pressures for the nonequilibrium cluster? In Ref. [3] it was suggested that the low-density depletion region around the growing crystal may serve to insulate the cluster from the pressure of the bulk liquid. In this section we shall derive expressions for the spatially varying normal and tangential components of the pressure tensor in the nonequilibrium crystal cluster which will be used in the following sections.

The osmotic pressure of a uniform crystalline or disordered suspension is given by Eq. (5). Uniformity here is defined locally as the vanishing of the first and second derivatives of the concentration. From the boundary conditions imposed above, we see that this condition will always apply at the surface $r=R$, so that

$$\pi(R)=\pi_0+\rho(R)\left.\frac{df}{d\rho}\right|_{r=R}-f[\rho(R)] \tag{15}$$

for all times.

In the presence of a radial nonuniformity, the osmotic pressure is a tensor with two distinct components

$$\Pi(r)=\pi_N(r)\mathbf{e}_r\mathbf{e}_r+\pi_T(r)[\mathbf{e}_\theta\mathbf{e}_\theta+\mathbf{e}_\phi\mathbf{e}_\phi], \tag{16}$$

where π_N and π_T are the scalar fields corresponding to the normal and tangential components, respectively, of the tensor field. In the case of local uniformity, as defined above, the normal and tangential components of the osmotic pressure are equal.

In general, the tangential component $\pi_T(r)$ can be written [12] as an extension of Eq. (5) to the case of a nonuniform density, i.e.,

$$\pi_T(r)=\pi_0+\rho(r)(\mu(r)-\mu_0)-\psi(r), \tag{17}$$

where $\mu(r)$ is the local chemical potential in the nonuniform system,

$$\begin{aligned}\mu(r)&=\mu_0+\frac{\delta F}{\delta\rho(r)}\\&=\mu_0+\frac{df}{d\rho}-\kappa^2\nabla^2\rho(r),\end{aligned} \tag{18}$$

and $\psi(r)$ is the local free-energy density

$$\psi(r)=f(\rho)+\frac{\kappa^2}{2}(\nabla\rho(r))^2. \tag{19}$$

Positive and negative deviations of $\pi_T(r)$ from the normal component of the osmotic pressure π_N correspond to compression and tension, respectively, in the inhomogeneous region.

The calculation of the normal osmotic pressure $\pi_N(r)$ is a somewhat more subtle issue [12]. In the case of the stationary clusters we must have mechanical equilibrium. The balancing of all forces which this equilibrium entails can be written as

$$\boldsymbol{\nabla}\cdot\Pi=\mathbf{0}. \tag{20}$$

Substituting Eq. (16) into this equation, we can write

$$\frac{d\pi_N}{dr}+\frac{2}{r}\pi_N(r)-\frac{2}{r}\pi_T(r)=0. \tag{21}$$

The result is a differential equation for $\pi_N(r)$, solvable once we know $\pi_T(r)$ [i.e., Eq. (17)] and the normal osmotic pressure at one point [e.g., $\pi(R)$ from Eq. (15)]. We are interested, however, in situations for which mechanical equilibrium does not apply.

Such a situation has already been considered in an earlier study [13] on the role of the density difference in crystal growth when acoustic modes, rather than diffusion, are the means of relaxing density inhomogeneities. There it was assumed that the nonequilibrium chemical potential could stabilize pressure gradients in the same way as an external field. Making use of this same approach, we shall write the nonequilibrium analog to Eq. (20),

$$\boldsymbol{\nabla}\cdot\Pi=-\rho(\mathbf{r})\boldsymbol{\nabla}\mu(\mathbf{r}), \tag{22}$$

which, for the case of the spherical cluster, becomes

$$\frac{d\pi_N}{dr}+\frac{2}{r}\,(\pi_N(r)-\pi_T(r))=-\rho(r)\,\frac{d\mu(r)}{dr}. \qquad (23)$$

This expression is used in the following sections to calculate the normal pressure component. Equation (23) has been integrated numerically from $r=0$ with $\pi_N(0)$ set equal to $\pi_T(0)$.

IV. STATIONARY CRYSTAL CLUSTERS

As a result of the reduced description of the hard-sphere crystallization by the concentration alone, we are restricted to looking at liquids whose uniform density is less than ρ_c $(=0.52)$. (A liquid above this density automatically becomes a low-density crystal when we only have density with which to distinguish the two phases.) The uniform density is always a stationary solution for a conserved order parameter. Two types of stationary nonuniform profiles are also possible. The thermodynamically stable phase for densities between the freezing density 0.495, and the upper bound 0.52 is the coexisting solid and liquid. With the assumption of radial symmetry, this appears as a spherical crystal cluster surrounded by liquid. Nucleation theory leads us to expect another stationary solution, an *unstable* one, representing the critical nucleus. We shall now see how these two nonuniform stationary solutions arise naturally from the time independent solutions of Eq. (1).

A stationary solution satisfies the equation $\delta F/\delta\rho(\mathbf{r})=\Delta\mu$, where $\Delta\mu=\mu-\mu_0$ and μ denotes a uniform chemical potential. This condition can be written as

$$\frac{df}{d\rho}-\kappa^2\,\frac{1}{r}\,\frac{\partial^2(r\rho)}{\partial r^2}=\Delta\mu. \qquad (24)$$

Note that this condition is equivalent to

$$\frac{d(f-\Delta\mu\rho)}{d\rho}-\kappa^2\,\frac{1}{r}\,\frac{\partial^2(r\rho)}{\partial r^2}=0, \qquad (25)$$

where the function $f(\rho)$ is replaced by $f-\Delta\mu\rho$—i.e., the conservation condition introduces an effective offset between the liquid and solid minima.

Thanks to the simple form of $f(\rho)$, we can write down the analytic expressions for the stationary profile $\rho(r)$ as a function of μ. Here we generalize the stationary solutions of Bagdassarian and Oxtoby [14] to the case of a finite confining radius R. The results of this earlier work [14] are recovered when $R\to\infty$. We divide the profile into an inner solution, for $\rho(r)>0.52$, and an outer solution for $\rho(r)<0.52$. The profile and its first derivative are required to be continuous at the boundary of the two regions, i.e., at $r=r_c$, where $\rho=\rho_c$. The stationary inner solution is

$$\rho(r)=\rho_s+\Delta\mu/\lambda_s+A/r(e^{-\alpha r}-e^{\alpha r}), \qquad (26)$$

where

$$A=(0.52-\rho_s-c/\lambda_s)\,\frac{r_c}{(e^{-\alpha r}-e^{\alpha r})}, \qquad (27)$$

$$\alpha=\sqrt{\lambda_s}/\kappa. \qquad (28)$$

The outer solution is

$$\rho(r)=\rho_l+\Delta\mu/\lambda_l+B/r(e^{-\beta r}-Ge^{\beta r}), \qquad (29)$$

where

$$G=\frac{e^{-2\beta R}(1+R\beta)}{(1-R\beta)}, \qquad (30)$$

$$B=(0.52-\rho_l-\Delta\mu/\lambda_l)\,\frac{r_c}{(e^{-\beta r}-Ge^{\beta r})}, \qquad (31)$$

$$\beta=\sqrt{\lambda_l}/\kappa. \qquad (32)$$

Stationary profiles are generated as follows. A value of r_c is selected. The matching condition for the first derivatives provides an expression for $\Delta\mu$ with respect to r_c,

$$\Delta\mu=\frac{E(r_c)[\rho_c-\rho_s]-[\rho_c-\rho_l]}{E(r_c)/\lambda_s-1/\lambda_l}, \qquad (33)$$

where

$$E(r_c)=\frac{1/r_c+\alpha(e^{-\alpha r_c}+e^{\alpha r_c})/(e^{-\alpha r_c}-e^{\alpha r_c})}{1/r_c+\beta(e^{-\alpha r_c}+Ge^{\alpha r_c})/(e^{-\alpha r_c}-Ge^{\alpha r_c})}. \qquad (34)$$

Values of $\Delta\mu$ and r_c are all that is required to generate the appropriate density profile from the equations above. The chemical potential determines a unique stationary profile. In order to determine the corresponding particle density, we simple integrate the density and divide by the total volume $4\pi R^3/3$. Finally, in order to present the results in the most general form, we have used the following reduced units:

$$\text{density:}\quad \rho=\frac{4\pi}{3}\,\rho^*\sigma^3,$$

$$\text{length:}\quad r=r^*\sqrt{\lambda}/\kappa,$$

$$\text{time:}\quad t=t^*D\lambda/\kappa^2,$$

where it is assumed that $\lambda_l=\lambda_s=\lambda$. Note that the superscript * denotes the actual or unreduced quantity. The reduced equation of motion is

$$\frac{\partial\rho(r,t)}{\partial t}=\frac{1}{r}\,\frac{\partial^2}{\partial r^2}\left(r(\rho(r,t)-\rho_\alpha)-\frac{\partial^2\rho(r,t)}{\partial r^2}\right). \qquad (35)$$

As r_c provides a useful measure of cluster size, we plot ρ vs r_c in Fig. 2 for a range of values of the confining radius R. The freezing and melting concentrations, along with ρ_c, are indicated. Systems with a concentration above 0.52 are not physically relevant here. [The two stationary solutions found above a concentration of 0.52 consist of the equilibrium phase (the smaller cluster) and the critical ''liquid'' fluctuation in the crystal (the larger cluster). The critical liquid fluctuation is artificially constrained to be the outer shell of the entire volume.]

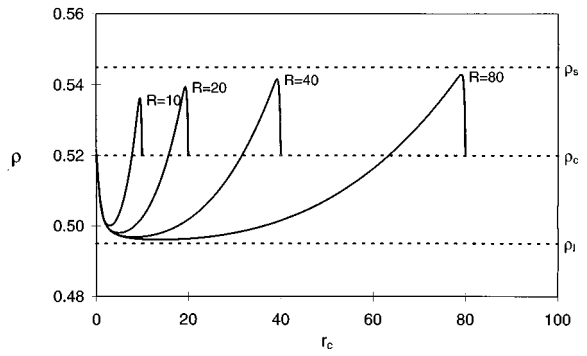

FIG. 2. The radius of stationary clusters r_c [defined as the radial distance at which $\rho(r_c)=\rho_c$] as a function of the overall concentration ρ for a range of values of the confining radius R. The freezing density ρ_l, the melting density ρ_s, and the crossover density ρ_c are indicated. As discussed in the text, only the cases with $\rho<\rho_c$ are of physical relevance here.

The results for $\rho<0.52$ clearly identify two stationary clusters per density over much of the accessible density range. Examples of the small and large cluster profiles at a single density are shown in Fig. 3. Note that a density gap exists between the freezing density and the first density at which a stationary nonuniform solution occurs. As we increase R, the radius of the confining volume, we see (in Fig. 2) that the large clusters grow, the density gap diminishes, and the small clusters are essentially unchanged.

We calculated the free energies of the three stationary solutions (small cluster, large cluster, and uniform density) as a function of ρ (see Fig. 4). Over most of the density range the magnitude of the free energies are ordered as follows:

large cluster<uniform density<small cluster.

From these results we identify the large cluster as the equilibrium crystal-liquid coexistence, and the small clusters as the unstable critical crystal nucleus. As the density decreases toward the freezing density, we find that the uniform free energy drops below that of the large cluster. Let this density be ρ_x. At a lower density still (ρ_g in Fig. 4) the large and small cluster solutions join and vanish, and we have the gap referred to above. As R increases, ρ_x and ρ_g converge rapidly to ρ_l.

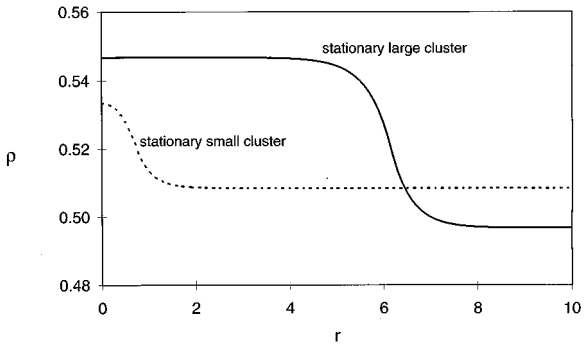

FIG. 3. The particle density profiles of the ''small'' and ''large'' stationary clusters at $\rho=0.5085$ and $R=10$. Note that the density at the center of the small cluster is less than that of the equilibrium crystal in coexistence with the disordered suspension.

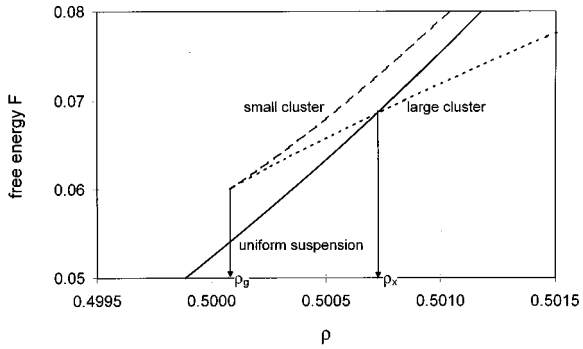

FIG. 4. The free energy of the small and large clusters and the uniform suspension as function of the overall concentration ρ for a confining radius of $R=10$. Over much of the concentration range the large cluster free energy lies below that of the uniform liquid, while the small cluster free energy lies above. At ρ_x the uniform liquid free energy drops below that of the large cluster, indicating the disappearance of stable coexistence between order and disorder. At an even lower density ρ_g we see the convergence and vanishing of both cluster solutions at a spinodal point.

The profiles of the normal and tangential components of the osmotic pressure have been calculated for the large and small stationary clusters at a total density $\rho=0.5085$ and plotted in Fig. 5. The sharp dip in the tangential component through the interface reflects the fact that the surface is under tension. The surface tension γ is simply the area enclosed between the two pressure profiles [12], i.e.,

$$\gamma=\int_0^\infty dr[p_N(r)-p_T(r)]. \tag{36}$$

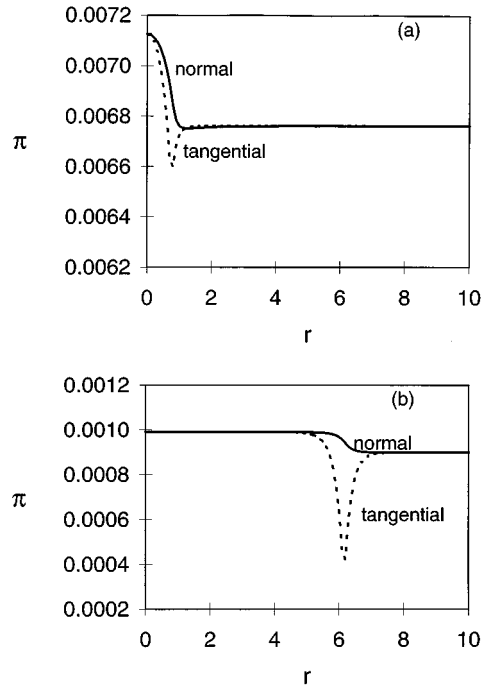

FIG. 5. The normal and tangential pressure profiles $\pi_N(r)$ and $\pi_T(r)$, respectively, calculated for (a) small and (b) large stationary clusters at a total concentration of $\rho=0.5085$ and $R=10$.

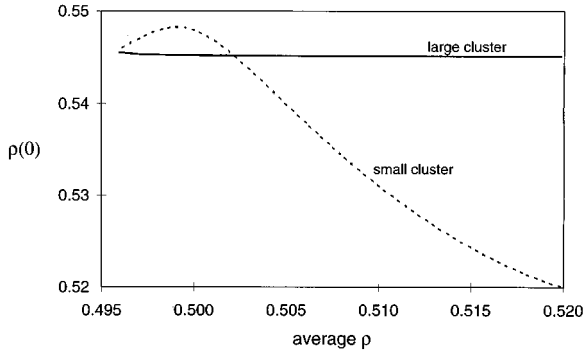

FIG. 6. The concentration at the center of the critical nucleus and the equilibrium crystal as a function of the overall concentration. Note that the critical nucleus concentration only exceeds the equilibrium value at very low concentrations.

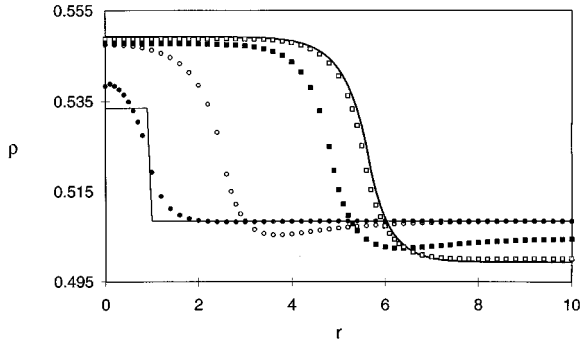

FIG. 7. Time dependence of the density profile of a growing cluster at $\rho=0.5085$ and with a confining radius of $R=10$. The different times (in time steps) are as follows: 10^5 (filled circles), 2×10^6 (empty circles), 4×10^6 (filled squares), 6×10^6 (empty squares), and 8×10^6 (solid line). The initial step profile cluster is also indicated by a solid line. Note the development of the depletion zone.

Note that, despite the fact that these stationary clusters are in mechanical equilibrium, there is a difference in normal osmotic pressure between the crystal and liquid phases as a consequence of the surface tension of the spherical interface [see Eq. (14)].

Having established the critical crystal nucleus and the equilibrium coexisting crystal and disordered suspension, we can make some preliminary observations about crystallization. *Assuming* that crystallization proceeds by the classic nucleation path, we have the initial and final states of the growth process. According to the behavior reported in Ref. [5], we would expect to see the crystal concentration in the critical nucleus to be considerably higher than that of the equilibrium crystal. In fact, we find the opposite for all but the suspension concentrations just above ρ_g, as shown in Fig. 6. Rather than seeing a *decreasing* crystal volume fraction during the course of growth, we find instead that the concentration at the center of the crystal must exhibit a net *increase* during growth from the critical nucleus. The intuition that the small crystallite is under compression is still correct, however, as can be seen in the comparison of the magnitudes of the osmotic pressure components at the center of the critical nucleus and the coexistence state in Fig. 5. The puzzling origin of this high pressure in the initial crystal cluster, in spite of a particle density lower than that of the equilibrium crystal, lies in the *nonclassical* treatment of the cluster by the field theory. The low crystal concentrations in the center of the critical nucleus is a consequence of the interfacial region extending into the center of the cluster. It is possible that the addition of a second-order parameter related to crystalline structure will alter this result.

V. DYNAMICS OF CRYSTAL CLUSTERS

From a range of starting clusters, we integrated the reduced equation of motion forward in time. The integration was carried out using an explicit Euler method with a time step of 0.000 01 and a radial step length of 0.1. The equation proved unstable to time steps much larger than this. As one of the checks of the algorithm, the solutions of Sec. IV were verified to be stationary.

In the absence of fluctuations in the equations of motion, we had to provide inhomogeneous starting states. Perturbations of the profile for the small stationary cluster proved to be very slow in developing in time. Smaller clusters were observed to rapidly shrink in time to reach, ultimately, the uniform disordered state. Larger clusters grew, developing a depletion region in the liquid adjacent to the advancing crystal interface, and finally coming to rest near the stationary large cluster solution. Early calculations exhibited a puzzling tendency to come to rest short of the stationary large cluster profile obtained analytically in Sec. IV. (Similarly, initial clusters larger than the appropriate stationary large cluster were found to stop before completely shrinking to the analytical form.) This problem was traced to the choice of the radial step length, Δr. As this was decreased the final structures approached the analytical result for large cluster. For the calculations reported here, we retained $\Delta r=0.1$.

A detailed discussion of the role of the initial profile and the implications for homogeneous nucleation has been left to Sec. VI. Here we focus on the time dependence of those crystal clusters which do grow to reach the equilibrium coexistence. In Fig. 7 we present snapshots of the density profile during crystal growth at $\rho=0.5085$. The short-time dynamics is dominated by the relaxation of the unstable square profile of the initial cluster. Note the appearance of a density depletion in front of the advancing interface at intermediate times. In Fig. 8 the square of the cluster radius r_c is plotted vs time for a number of different densities. We find that the

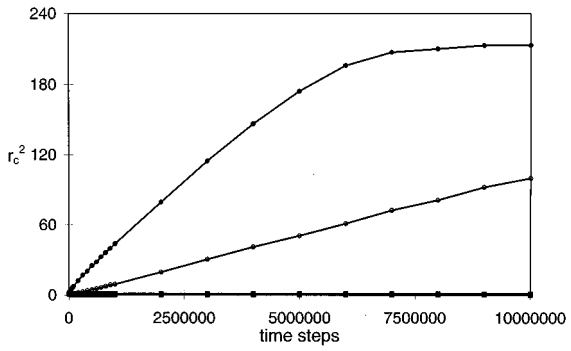

FIG. 8. Time dependence of the cluster radius squared r_c^2 for three densities: 0.5180, 0.5085, and 0.5030, in order of decreasing crystallization rates. The growth is linear in time over the intermediate time interval indicating a $t^{1/2}$ growth law.

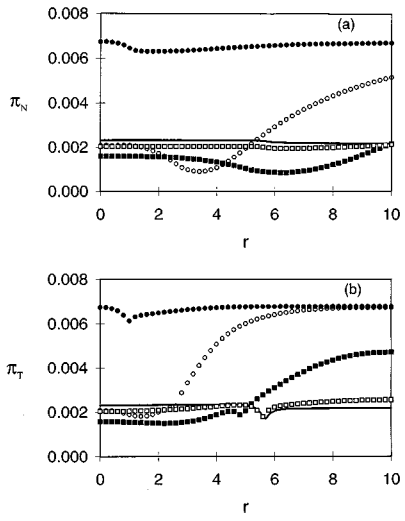

FIG. 9. Time dependence of the osmotic pressure fields (a) $\pi_N(r)$ and (b) $\pi_T(r)$ about a growing crystal at $\rho=0.5085$ and with $R=10$. The various times are indicated as in Fig. 7. Note the rapid decrease of normal and tangential components in the crystal region.

square of the cluster radius grows linearly with time over the period between the relaxation of the initial cluster, and the final slowing down as the equilibrium coexistence is approached, i.e., we have a $t^{1/2}$ growth law. We were unable to observe any crossover to a linear growth law at low concentrations. The lack of observable growth at $\rho=0.503$ is a result of the slow dynamics we observe around the critical nucleus. The rapid relaxation of the initial cluster tends to leave them with a profile close to that of the critical nucleus.

We calculated the normal and tangential osmotic pressure fields in the nonequilibrium system of the growing crystal cluster at a total concentration of $\rho=0.5085$ and plotted the results in Fig. 9. Both components of the pressure exhibit a rapid decrease in magnitude in the crystalline region, while the disordered suspension persists at a high pressure. This initial decrease is the result of the development of a depletion zone which has isolated the crystal from the surrounding suspension, just as Ackerson and Schätzel suggested [3]. The osmotic pressure fields then proceed with a slow propagation of the crystal and its depletion zone out into the disordered suspension, leading to a decrease in its osmotic pressure. The results are quite striking. Rather than a steady decrease in the crystal pressure during the entire course of crystallization as suggested by the experimental work of Harland and van Megen [5] and the theoretical model of Ref. [3], we find instead that the crystal completes its pressure drop very rapidly, well before the osmotic pressure in the disordered state has had much chance to change.

VI. ON THE NATURE OF NUCLEATION UNDER CANONICAL CONSTRAINTS

The space of possible clusters is infinite, thanks to the continuum description via the density function. In order to provide a picture of the nucleation behavior, we chose to restrict possible clusters to the shape shown in Fig. 10. Each cluster can be identified at a given density by two variables, the radius r_c and the depletion depth Δ. We used interfaces

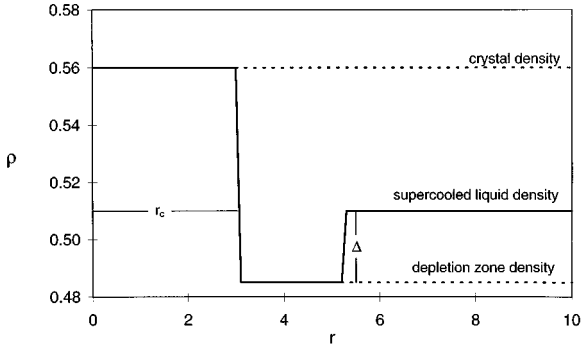

FIG. 10. The generic initial cluster profile used in the time-dependent calculations. In this paper we have chosen to set the crystal concentration to 0.56 and the disordered suspension concentration to 0.51. The radius r_c and depletion depth Δ are then varied so as to ensure that the overall concentration is satisfied.

of finite width here in order to be able to calculate free energies of the clusters. The fates of the various clusters at $\rho=0.5085$ are indicated in Fig. 11. Open circles indicate the cluster eventually disordered while close circles indicate eventual ordering. The boundary between the open and closed circles indicates some sort of transition state in the reduced space of cluster shapes considered here. Note that the critical radius increases with increasing depth of the depletion region due to the tendency of this depletion to induce transient melting.

Calculations of the time-dependent free energies of clusters as they either order or disorder shows that the free energy decreases monotonically with time for either process. This is consistent with the transition state identified in Fig. 11 corresponding to a loci of maxima in the cluster free energy with respect to cluster radii. The interesting feature, however, is that the free energy of the initial cluster have no extrema corresponding to this line. In fact, the initial cluster free energy have *no* extrema over the entire space studied. (The cluster free energy was found to decrease monotonically with increasing initial radius. This is a result of the

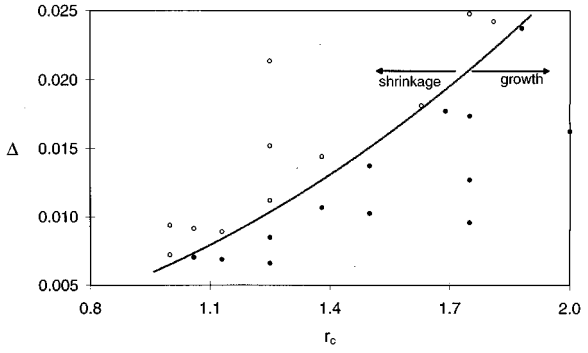

FIG. 11. Map of the fates of initial clusters. Initial clusters, characterized by a pair of values r_c and Δ, which go on to crystallize, are indicated by a filled circle. Clusters which melt are indicated by an empty circle. As discussed in the text, the dividing line between growth and melting does *not* correspond to a maximum in the initial cluster free energy. Note that the critical radius increases as the initial depletion region becomes deeper and narrower.

steep step profile chosen for the initial cluster. The resulting large surface tension of this profile dominates the cluster free energy.) This apparent inconsistency is a consequence of the difference between the extremely reduced space of cluster shapes, i.e., (r_c,Δ), which we have introduced in order to try and describe the possible initial clusters, and the much larger space of actual clusters accessible to the dynamical process. Any ''real'' transition state exists in this complete space of clusters. The ''watershed'' divide we see in Fig. 11 between the open and closed circles is presumably the projection of this transition surface down onto the reduced two-dimensional space with no reason for this projection to represent local maxima. This result can be taken as a general caution: if you would like to apply classical nucleation theory to describe cluster ''fates'' within a reduced space of constrained initial clusters, then you must ensure that the equations of motion for those clusters incorporate the same constraints.

VII. DISCUSSION

In this paper we have presented a preliminary study of crystallization in a hard-sphere colloidal suspension. The study is preliminary in the sense that a number of physical features important for the colloidal crystallization problem (i.e., structural order parameters, accurate free energies, and density-dependent diffusion constants) have been omitted in order that the fundamental aspects of the constraint on N and V can be clearly viewed. We intend to include these aspects in future papers. We have developed a microscopic description capable of treating the effect of density conservation on the dynamics of the crystal cluster, the time dependence of the nonuniform osmotic pressure field, and the nonuniform stationary and equilibrium states, all within a single consistent formalism. While limited by the lack of crystalline order parameters to densities just above the freezing density, we have presented two important formal developments: the determination of the stationary nonuniform states under the constraint of fixed N and V, and the expressions for the time-dependent components of the pressure tensor.

We have shown that the freezing transition is perturbed to higher concentrations as a result of the small confining volumes. This can be understood as the critical nuclei at low concentrations being too large to fit within the restricted space. We recall that the confining volume was introduced to model, in a mean-field sense, the effect of competing crystal clusters in a bulk suspension. This perturbation of the freezing transition due to ''confinement'' by surrounding growing clusters would be expected to suppress nucleation during the later stages of growth. The crystal radius was found to increase as $t^{1/2}$ over times intermediate between the initial transient behavior and the final relaxation to the equilibrium state. Examination of the osmotic pressure fields about the growing crystal indicate that, through the development of a depletion zone, the crystal pressure drops quite quickly to a value close to the final equilibrium value. The pressure decrease out in the disordered suspension takes considerably longer, waiting upon the propagation of the interface.

The time dependence of the density of the crystal cluster appears to be at odds with that reported by Harland and van Megen [5] and the model calculations of Ackerson and Schätzel [3]. Both groups described a crystal density which decreases steadily as crystallization proceeds, with the decompression of the crystal cluster being largely slaved to the extent of crystallization. In contrast, over the limited density range of our results we find that the crystal density in the critical nucleus is *less* than that of the equilibrium crystal for most of the density range and, following some fast relaxation of the initial cluster, we see a small but steady *increase* in the density at the cluster center. These features have been identified with the ''nonclassical'' description of the nucleus in which the interface between order and disorder is treated continuously. It remains to be seen how the incorporation of structural order parameters into the density functional theory changes this picture. Work on this problem is continuing.

ACKNOWLEDGMENTS

We gratefully acknowledge valuable discussions with Amalia Stone, Bill van Megen, Bruce Ackerson, and Stuart Henderson, and thank Bill van Megen for providing a preprint of Ref. [5]. This work was supported by Grant No. A2930072 from the Australian Research Council.

[1] J. K. G. Dhont, C. Smits, and H. N. W. Lekkerkerker, J. Colloid Interface Sci. **152**, 386 (1992).
[2] K. Schätzel and B. J. Ackerson, Phys. Rev. E **48**, 3766 (1993).
[3] B. J. Ackerson and K. Schätzel, Phys. Rev. E **52**, 6448 (1995).
[4] J. L. Harland, S. I. Henderson, S. M. Underwood, and W. van Megen, Phys. Rev. Lett. **75**, 3572 (1995).
[5] J. L. Harland and W. van Megen, Phys. Rev. E **55**, 3054 (1997).
[6] A. Stone, Honours thesis, University of Sydney, 1993.
[7] H. A. Wilson, Philos. Mag. **50**, 238 (1990); J. Frenkel, *Kinetic Theory of Liquids* (Oxford University Press, Oxford, 1946).
[8] R. Evans, Adv. Phys. **28**, 143 (1979).
[9] J. W. Cahn and J. E. Hilliard, J. Chem. Phys. **31**, 688 (1959).
[10] J. Tobochnik and P. M. Chapin, J. Chem. Phys. **88**, 5824 (1987).
[11] B. J. Alder, W. G. Hoover, and D. A. Young, J. Chem. Phys. **49**, 3688 (1968).
[12] J. S. Rowlinson and B. Widom, *Molecular Theory of Capillarity* (Clarendon, Oxford, 1982).
[13] D. W. Oxtoby and P. Harrowell, J. Chem. Phys. **96**, 3834 (1992).
[14] C. K. Bagdassarian and D. W. Oxtoby, J. Chem. Phys. **103**, 2139 (1994).